Low frequency depolarized Raman spectra in water: Results from normal mode analysis

Srikanth Sastry[a] and H. Eugene Stanley
Center for Polymer Studies and Department of Physics, Boston University, Boston, Massachusetts 02215

Francesco Sciortino
Dipartimento di Fisica, Universitá di Roma La Sapienza, Piazzale Aldo Moro, Rome, Italy 00185

(Received 15 November 1993; accepted 26 November 1993)

The Raman spectrum of water in the translational frequency regime has been interpreted in terms of localized vibrational density of states and, in seeming contradiction, in terms of contributions of long-range dipole induced dipole (DID) reactions. We show that these interpretations can be consistently understood by obtaining the Raman spectrum from the normal modes of the inherent liquid structures. We calculate the DID contributions to the Raman spectra for each individual mode, and show that the aggregate spectrum obtained agrees well with both the DID spectrum obtained directly from a molecular dynamics simulation and the spectrum obtained by simulating harmonic dynamics (i.e., exciting all the modes at once and calculating the DID spectrum from the resulting dynamical trajectory of the system).

I. INTRODUCTION

Raman spectra for water in the translational vibration region have been studied experimentally by many groups.[1–4] More recently, Raman spectra have been calculated numerically[5–9] for water and for hexagonal ice.[10] The numerical calculations have been valuable in their ability to separate the various contributions to the spectra observed experimentally, thus leading to the identification of features in the spectra with specific mechanisms.

In particular, the depolarized Raman spectrum in the low frequency region has been shown to be dominated by the DID (dipole induced dipole) collision contributions. The low frequency peaks around 60 and 180 cm^{-1} observed in experiments[1–3] have been shown to arise principally from DID contributions.[8] This observation, however, has been considered[8] to be contrary to previous interpretations of these peaks[1–3] in terms of localized vibrational excitations of molecules.

In this paper, we present results showing that these two interpretations can be understood consistently by comparing the DID Raman spectra calculated from molecular dynamics (MD) simulations of the liquid state and of the corresponding harmonic quenched structures (inherent structures). Specifically, we calculate from an MD simulation the depolarized DID spectrum. We then calculate the corresponding spectrum from the normal modes of quenched configurations; i.e., from configurations obtained by minimizing the potential energy of configurations equilibrated in the MD run (applications of normal mode analysis to the study of simple liquids and water may be found in Refs. 11–14). We show that the significant features of the liquid spectrum are captured in the spectrum obtained from the normal modes. Further, we show that the normal mode spectrum bears a close relation to the normal mode density of states (DOS). Hence, while the detailed mechanism for the scattering is the DID interaction, the vibrational DOS determines the observed spectrum to a large extent.

We use the TIP4P potential for water,[15] which has been shown to be able to reproduce satisfactorily many thermodynamic properties of water. Further, simulation studies directed specifically at obtaining Raman spectra of water using TIP4P have shown TIP4P to be satisfactory.[9]

In Sec. II, we describe the details of the MD simulation, the procedure used for quenching and the method whereby the normal modes and the DOS are obtained. In Sec. III, we describe how we calculate the Raman spectra from the MD run and the normal modes respectively. In Sec. IV, we present and discuss the results. In Sec. V, we discuss the conclusions arising from our work.

II. COMPUTATIONAL DETAILS

The MD simulation is performed for a system of 216 molecules in a cubic box of side 1.89 nm, corresponding to a density of 1 gm/cm^3. Molecules interact via the TIP4P potential,[15] a two-body rigid-molecule potential previously used to study Raman spectra.[8] After equilibrating the system in the NVT ensemble at 235 K using the Berendsen algorithm,[16] the simulation was performed in the NVE potential for obtaining the configuration trajectory. The integration time step was 1 fs and the equilibrated configurations were saved every 25 fs, for a total length of 400 ps. The stored coordinates are used to obtain the Raman spectra as described in the next section.

Sixteen equally spaced configurations from the MD run were then selected and quenched to their closest local minima by decreasing the temperature gradually to 0 K.[17] This procedure has been tested to ensure that the initial configuration loses kinetic energy gradually and reaches the closest potential energy minimum. That the resulting configuration is a potential energy minimum can be verified by the absence of any negative eigenvalues when the normal mode calculation is performed.

[a]Present address: Physical Science Laboratory, Division of Computer Research and Technology, NIH, Bethesda, MD 20892.

 0021-9606/94/100(7)/5361/6/$6.00

In the configurations thus obtained, which are referred to as *quenched* configurations henceforth, each coordinate experiences a harmonic potential for small oscillations. Then, the potential energy is well described by keeping only terms of quadratic order in the Taylor expansion,

$$V(x_i,\ldots,x_N)=V(x_{0i},\ldots,x_{0N})+\frac{1}{2}\left(\frac{\partial^2 V}{\partial x_i\,\partial x_j}\right)_0 x_i x_j+\cdots, \tag{2.1}$$

where the subscript 0 refers to the equilibrium positions of all the coordinates x_i.

To obtain the normal modes, we diagonalize the Hessian matrix of second derivatives,

$$\mathscr{H}_{ij}=\left(\frac{\partial^2 V}{\partial x_i\,\partial x_j}\right)_0. \tag{2.2}$$

For the TIP4P potential, the Hessian matrix is defined for the set of $6N$ coordinates of the N water molecules, with $3N$ of the coordinates being center of mass coordinates and $3N$ coordinates being rotational coordinates. The normalized coordinates $x_{i\alpha}^{\mathrm{COM}}$ of the center of mass (COM) are given in terms of actual COM coordinates $X_{i\alpha}$ by

$$x_{i\alpha}^{\mathrm{COM}}=M^{1/2}X_{i\alpha}, \tag{2.3}$$

where i labels the molecule and α labels the Cartesian component. M is the molecular mass. Similarly, the normalized rotational coordinates $x_{i\alpha}^{\mathrm{ROT}}$ are given in terms of the angular position $\Omega_{i\alpha}$ with respect to the αth principal axis by

$$x_{i\alpha}^{\mathrm{ROT}}=I_\alpha^{1/2}\Omega_{i\alpha}, \tag{2.4}$$

where I_α is the momentum of inertia for that principal axis. The principal axes for the TIP4P water molecule are (i) perpendicular to the plane of the molecule, (ii) the bisector of the H–O–H angle and, (iii) the axis perpendicular to the first two.

The Hessian matrix is calculated numerically, by making small displacements along each of the normalized coordinates $x_{i\alpha}^{\mathrm{COM}}$ and $x_{i\alpha}^{\mathrm{ROT}}$. The matrix thus obtained is diagonalized using a standard numerical diagonalization package. The resulting eigenfunctions and eigenfrequencies are stored for further calculations of the "configuration-averaged" DOS and of the Raman spectrum.

III. RAMAN SPECTRA

The Raman spectra can be calculated from the Fourier transform of the time-dependent macroscopic polarizability $\vec{\vec{P}}$ which is decomposed into the isotropic part P_{iso} and the depolarized part P_{dep}, given by

$$I_{\mathrm{iso}}(t)=\frac{1}{3}\sum_{\alpha=1}^{3} P_{\alpha\alpha}, \tag{3.1}$$

and

$$I_{\mathrm{dep}}(t)=\frac{1}{10}\sum_{\alpha\beta=1}^{3}[P_{\alpha\beta}-\delta_{\alpha\beta}I_{\mathrm{iso}}(t)]. \tag{3.2}$$

In a molecular system, $\vec{\vec{P}}$ can be written as a sum of point polarizabilities over all the N molecules in the scattering volume. For each component of the tensor $\vec{\vec{P}}$ we have $P_{\alpha\beta}=\Sigma_{i=1}^{N}P_{\alpha\beta}^{i}$, where

$$P_{\alpha\beta}^{i}\equiv\lim_{E^o\to 0}\frac{\partial\mu_\alpha^i}{\partial E_\beta^o}, \tag{3.3}$$

is the $\alpha\beta$ component of the polarizability tensor of molecule i, $\mathbf{E}^o$ is the electric field of the incident laser beam, and $\boldsymbol{\mu}^i$ is the effective dipole moment on molecule i (i.e., sum of the permanent, $\boldsymbol{\mu}^{io}$, and of the induced dipole). Taking into account only the molecular polarizabilities and following Refs. 7–9 $\boldsymbol{\mu}^i$ can be expressed in terms of the local electric field on the ith molecule, i.e., the sum of the electric field of the incident laser beam plus the electric field generated by all the other molecules in the system, as

$$\mu_\alpha^i=\mu_\alpha^{io}+\alpha_{\alpha\beta}^i E_\beta+\frac{1}{3}A_{\alpha,\beta\gamma}^i E'_{\beta\gamma}++\cdots, \tag{3.4}$$

where E_α and $E'_{\alpha\beta}$ stand for the Cartesian components of the electric field and its gradient, α is the molecular bare polarizability, and A is the dipole–quadrupole polarizability.

From these equations, $P_{\alpha\beta}^i$ can be written as the sum of the bare polarizability, $\alpha_{\alpha\beta}^i$, plus an interaction induced contribution, which depends only on (i) the electronic properties of each isolated molecule and (ii) the relative distance $|\mathbf{R}_{ij}|$ of all the pairs ij of molecules in the system. The electric field on molecule i produced by the n pole of molecule j [see Eq. (3.4)] is a function of $|\mathbf{R}_{ij}|$ given in terms of the n-pole propagator,

$$T^{(n)}{}_{\alpha_1,\ldots,\alpha_n}(ij)=(-1)^n\nabla_{\alpha_1}\cdots\nabla_{\alpha_n}|\mathbf{R}_{ij}|^{-1}. \tag{3.5}$$

Keeping only the first order term in $T^{(n)}(ij)$ for the dipole induced dipole, we have,

$$P_{\alpha\beta}^i=\alpha_{\alpha\beta}+\sum_{j\neq i}\alpha_{\alpha\gamma}^i T_{\gamma\delta}^{(2)}(ij)\alpha_{\delta\beta}^j+\cdots. \tag{3.6}$$

The first term in Eq. (3.6) describes the response to the external field on i. It gives rise to a depolarized contribution, strictly related to the single-molecule rotational motion, i.e., mainly in the region above 400 cm^{-1}.

The second term describes how the changes induced by the external field on molecule j propagate to molecule i via the polarizability of molecule j. This term, related to the collective molecular modes, has been shown to be the leading contribution in the translational frequency region we are interested in. For this reason, we consider only the DID [second term in Eq. (3.6)] in the present work. Further, we treat only the isotropic part of the polarizability tensor α, since the inclusion of the nondiagonal components does not produce significant contributions in the depolarized spectrum.[18]

The DID polarizabilities of isotropic scatterers (IDID) are thus given by

$$P_{\alpha\beta}=\alpha^2\sum_i\sum_{j\neq i}T_{\alpha\beta}^{(2)}(ij), \tag{3.7}$$

where $\alpha\equiv(\alpha_{11}+\alpha_{22}+\alpha_{33})/3$ and

$$T^{(2)}_{\alpha\beta}(ij)=3R_{ij\alpha}R_{ij\beta}/|\ \mathbf{R}_{ij}|^5. \tag{3.8}$$

We use the molecular polarizabilities given in units of Å^{-3} by $\alpha_{11}=1.47$, $\alpha_{22}=1.528$, and $\alpha_{33}=1.468$ (from Refs. 19 and 20). Equation (3.7) is the basic equation for the results described below. The time evolution of the IDID polarizabilities is obtained from the time evolution of intermolecular distances through Eq. (3.8).

Note that the structure of the propagator $T^{(2)}_{\alpha\beta}(ij)$ is a nonlinear function of the intermolecular distance. Thus, even for a system with oscillations at a single frequency ω, the spectrum of the polarizability will contain contributions at ω, 2ω, 3ω,.... In the case of a system undergoing harmonic motion with many frequencies, the polarizability spectrum will have a contribution from each of the excited modes plus all the overtones and all the couplings between the modes. The IDID Raman spectrum can be stated to have a strong relationship to the DOS only if the contribution from overtones and couplings can be neglected compared to the *single mode* contribution.

We describe here how the spectrum is calculated from normal modes. We start by writing the time-dependent position $x_{i\alpha}$ of a given molecule i along the Cartesian axis α as,

$$x_{i\alpha}(t)=x^o_{i\alpha}+\sum_n a_{i\alpha,n}\xi_n(t)\equiv x^o_{i\alpha}+\delta x_{i\alpha}, \tag{3.9}$$

where $a_{i\alpha,n}$ is the component of the normal mode n along $i\alpha$. From the above expression, one obtains the components of the time-dependent distance R_{ij} separating molecules i and j, as,

$$R_{ij\alpha}(t)=(x^o_{i\alpha}-x^o_{j\alpha})+(\delta x^o_{i\alpha}-\delta x^o_{j\alpha})\equiv R^o_{ij\alpha}+\delta R_{ij\alpha}. \tag{3.10}$$

The amplitude and time variation of each normal mode ξ_n is given by,

$$\xi_n(t)=\xi_{no}\cos(\omega_n t+\delta_n);\quad \xi_{no}=\frac{(2k_BT)^{1/2}}{\omega_n}, \tag{3.11}$$

where ω_n is the frequency of the mode, k_B is the Boltzmann constant, and δ_n is a random phase shift for the mode n and T is the temperature, chosen in the following calculations to be the same as the temperature of the MD simulation. The amplitude ξ_{no} is chosen so as to satisfy the equipartition theorem for the average energy per degree of freedom.

From Eqs. (3.10)and (3.8), we obtain $P_{\alpha\beta}(t)$ [given by Eq. (3.7)] from which the total normal mode spectrum is calculated numerically.

For low temperatures, treating the displacements δR_{ij} as small compared to the equilibrium distances R_{ij}, the denominator in (3.8) can be Taylor expanded and $P_{\alpha\beta}$ in turn can be written as a sum of successive contributions arising from couplings of different number of normal modes:

$$P_{\alpha\beta}(t)=P^{(0)}_{\alpha\beta}+P^{(1)}_{\alpha\beta}(t)+P^{(2)}_{\alpha\beta}(t)+\cdots, \tag{3.12}$$

with

$$P^{(0)}_{\alpha\beta}=3\alpha^2\sum_{i,j\neq i}R^o_{ij\alpha}R^o_{ij\beta}/R^{o5}_{ij}, \tag{3.13}$$

$$P^{(1)}_{\alpha\beta}(t)=\sum_n \tilde{P}^1_{\alpha\beta n}\cos(\omega_n t+\delta_n), \tag{3.14}$$

and

$$P^{(2)}_{\alpha\beta}(t)=\sum_{n,n'}\tilde{P}^{(2)}_{\alpha\beta,nn'}[\cos((\omega_n+\omega_{n'})t+\delta'_{nn'}) +\cos((\omega_n-\omega_{n'})t+\delta''_{nn'})]. \tag{3.15}$$

Here,

$$\tilde{P}^{(1)}_{\alpha\beta,\,n}=3\alpha^2\sum_{i,j\neq i}R^{o\ -5}_{ij}\left\{R^o_{ij\alpha}\delta R^o_{ij\beta,n}+R^o_{ij\beta}\delta R^o_{ij\alpha,n} -\frac{5}{R^{o\ 2}_{ij}}\sum_{\gamma=1,3}R^o_{ij\alpha}R^o_{ij\beta}R^o_{ij\gamma}\delta R^o_{ij\gamma,n}\right\}, \tag{3.16}$$

and,

$$\tilde{P}^{(2)}_{\alpha\beta,nn'}=3\alpha^2\sum_{i,j\neq i}\left\{\frac{\delta R^o_{ij\alpha,n}\delta R^o_{ij\beta,n'}}{R^{o\ 5}_{ij}}-\frac{5}{4R^{o\ 7}_{ij}}R^o_{ij\alpha}R^o_{ij\beta}\sum_{\gamma=1,3}R^{o\ 2}_{ij\gamma}\,\delta R^o_{ij\gamma,n}\,\delta R^o_{ij\gamma,n'}-\frac{5}{2RR^{o\ 7}_{ij}}\sum_{\gamma=1,3}R^o_{ij\alpha}R^o_{ij\gamma}\delta R^o_{ij\beta,n}\delta R^o_{ij\gamma,n'} -\frac{5}{2R^{o\ 7}_{ij}}\sum_{\gamma=1,3}R^o_{ij\beta}R^o_{ij\gamma}\delta R^o_{ij\alpha,n}\delta R^o_{ij\gamma,n'}+\frac{35}{4R^{o\ 9}_{ij}}R^o_{ij\alpha}R^o_{ij\beta}\sum_{\gamma,\ \eta=1,3}R^o_{ij\gamma}R^o_{ij\eta}\delta R^o_{ij\gamma,n}\delta R^o_{ij\eta,n'}\right\}. \tag{3.17}$$

Of the above contributions, $P^{(0)}_{\alpha\beta}$ is time independent and does not contribute to the spectrum. Each term with a different frequency in $P^{(1)}_{\alpha\beta}(t)$ and $P^{(2)}_{\alpha\beta}(t)$ contributes separately to the power spectrum (i.e., no cross terms) since the cosines are orthogonal functions. Further, even terms in $P^{(1)}_{\alpha\beta}(t)$ and $P^{(2)}_{\alpha\beta}(t)$ which have the same frequency contribute independently since each normal mode has a random phase which lead to the cancellation of products between such terms when the phases are averaged. Thus, the terms in Eq. (3.12) contribute additively to the power spectrum of $P_{\alpha\beta}(t)$ when averaged over phases of the modes. In particular, considering only $P^1_{\alpha\beta}$, we can calculate the contributions to the total spectrum wherein no couplings between normal modes are present. The single-mode spectrum is calculated in this fashion, using only $P^{(1)}_{\alpha\beta}(t)$ (or, equivalently, binning $\tilde{P}^{(1)}_{\alpha\beta}$ in frequency). The second order spectrum is calculated using $P^{(2)}_{\alpha\beta}(t)$.

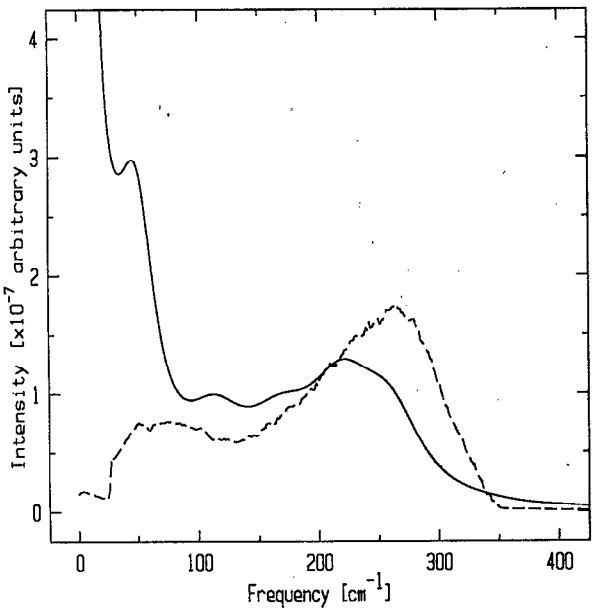

FIG. 1. The full line shows the IDID spectrum from the MD simulation at 235 K; two finite-frequency peaks are seen, at 50 and 230 cm^{-1}. The dashed line shows the IDID total normal mode spectrum obtained by exciting one normal mode at a time; two finite-frequency peaks are seen, at 60 and 270 cm^{-1}. The temperature used in the normal mode calculation is the same as that of the MD simulation. The y scale is arbitrary.

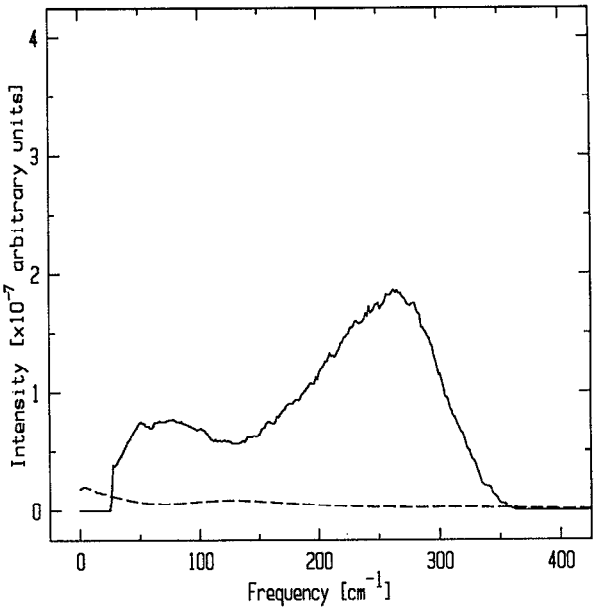

FIG. 2. The full line shows the IDID single-mode spectrum obtained by exciting all the normal modes; two finite-frequency peaks are seen, at 60 and 270 cm^{-1}, as in Fig. 1. The single-mode spectrum shown here is almost the same as the total normal mode spectrum shown in Fig. 1. The dashed line shows the second-order spectrum which is the leading correction to the single-mode spectrum. Note that the second order spectrum makes a negligible contribution. The y scale is arbitrary, and the same as in Fig. 1.

IV. RESULTS AND DISCUSSION

As shown in the previous section, only the power spectrum of $P^{(1)}_{\alpha\beta}(t)$ is proportional to the DOS, with an ω dependent proportionality factor which controls the Raman activity of the mode. Analogously, the power spectrum of $P^{(2)}_{\alpha\beta}(t)$ can be seen as a ω-weighted convolution of the DOS with itself. *If, and only if* the contributions of order higher than 1 can be neglected, can the interpretation of the *total* Raman spectra in the translational region in terms of collective modes be justified.

To study if this is the case for liquid water, we first compare the spectrum when the time evolution of the intermolecular distance is calculated from (a) the MD simulation and (b) from the harmonic dynamic using as reference state each of the quenched configurations [i.e., calculating the time evolution of the intermolecular distances according to Eq. (3.10)].

Figure 1 shows the MD spectrum along with the total normal mode spectrum. The MD spectrum exhibits two clearly visible finite frequency peaks. The lower peak is at roughly 50 cm^{-1} and is fairly sharp. The higher peak at roughly 230 cm^{-1} is considerably broader.

The normal mode spectrum, shown on the same scale, again exhibits two well-defined peaks, centered at slightly higher frequencies respect to the MD spectrum. As expected, the intense signal close to zero frequency observed in the MD spectrum is not found in the normal mode spectrum due to the absence of diffusional processes in the quenched system from which the normal mode spectrum is obtained. This difference, however, does not affect our analysis which is focused on the physical origin of the 50 and 230 cm^{-1} peaks.

Note also that the peak positions in the normal mode spectrum are shifted to slightly higher frequencies compared to the MD case.[21] This shift is also expected and arises (i) due to the difference in temperature (finite temperature in the MD simulation as compared with the zero temperature of the quenched state); and (ii) due to the damping of underlying oscillations in the case of the liquid (i.e., MD simulation) related to hopping between potential energy minima. Such damping of the underlying normal mode oscillations produces a broadening of the frequency distribution and a low frequency shift. For details see, e.g., Ref. 13.

The fact that the spectrum calculated in the harmonic approximation (i.e., from quenched configurations) maintains the same spectral feature of the liquid state we are interested in allows us to apply the powerful formalism of the normal modes to the problem. As described in the previous section, for quenched configurations it is possible to calculate exactly the contributions from different orders. Specifically, by comparing the single mode spectrum and the DOS, we can estimate the influence of vibrational modes on the depolarized Raman spectrum.

Figure 2 shows the first order approximation to the Raman spectrum. It is clear from Figs. 1 and 2 that the total normal mode spectrum is essentially the same as the single-mode spectrum. To illustrate this point further, we also show in Fig. 2 the second order spectrum, which is the leading correction to the single-mode spectrum in the full expression of the total normal mode spectrum. The correction due to the second order spectrum is quite negligible for most of the

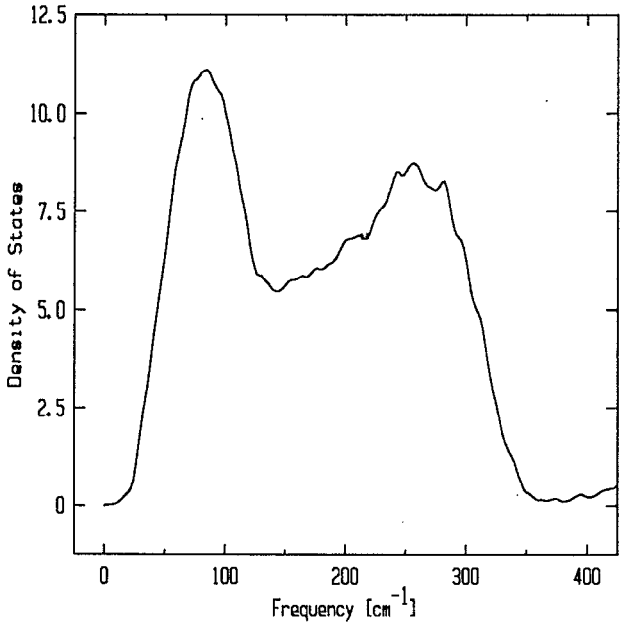

FIG. 3. The configuration averaged DOS for the quenched configurations, averaged over 16 equilibrium configurations obtained by minimizing the potential energy of instantaneous MD configurations. The DOS contributions below 400 cm^{-1} arise from the COM degrees of freedom (translational) while the contributions above 400 cm^{-1} are from rotational degrees of freedom (librational). Only the translational frequency range is shown here.

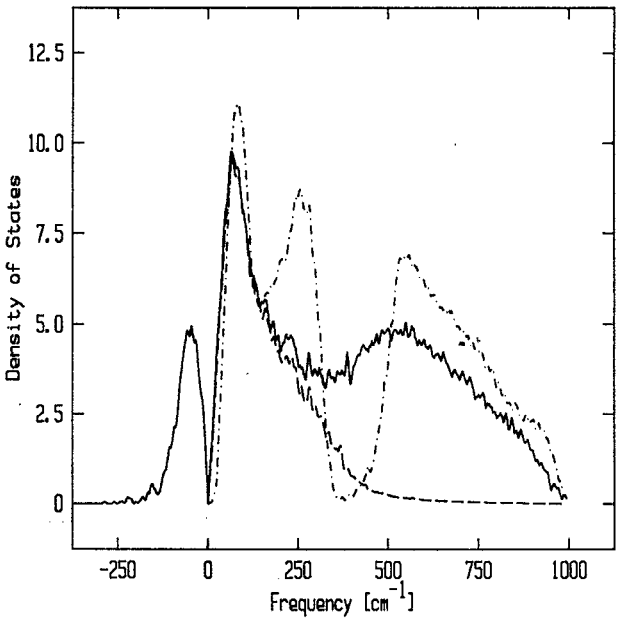

FIG. 5. The full line shows the configuration averaged DOS for finite temperature configurations at 235 K, obtained from instantaneous configurations MD configurations. The dashed line shows the translational part of the DOS at finite temperature 235 K, obtained by calculating the contribution of the COM coordinates to each mode. The zero temperature DOS is also shown for comparison (dot–dashed line). Note the absence of a peak at 280 cm^{-1} in the finite temperature DOS. Also note that there is no clear separation between translational and rotational (librational) parts.

frequency range shown. Hence, we see that the single-mode spectrum is a very accurate estimate of the full spectrum in the harmonic approximation.

To further illustrate the relation between the Raman spectrum and the DOS (shown in Fig. 3), we show in Fig. 4

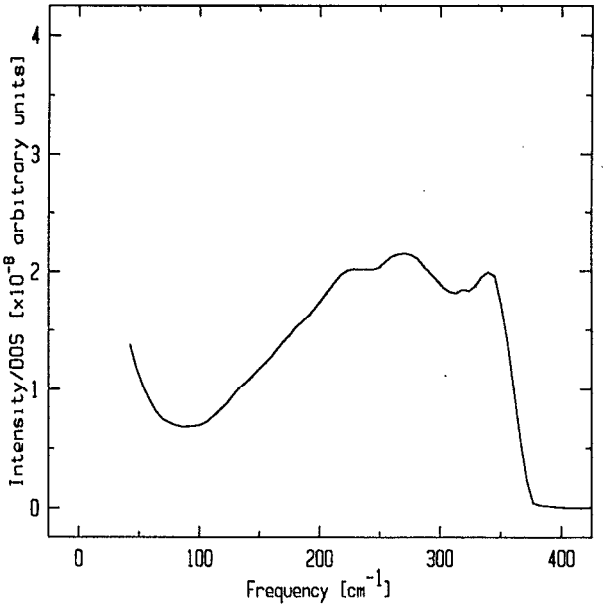

FIG. 4. IDID single-mode spectrum in Fig. 2 divided by the quenched density of states (Fig. 3). Note that the ratio between the spectrum and the DOS is not constant but shows a broad "bump" around 270 cm^{-1}. The y scale is arbitrary.

the ratio of the calculated single mode Raman intensity and the DOS. We see that the ratio is not constant and has a broad bump centered around 270 cm^{-1}. Thus, different modes are "Raman-active" to different degrees, and hence the frequency position of peaks may be different between DOS and Raman spectra. However, the peaks present in the normal mode spectrum arise directly from the features of the DOS. In other words, although the intensity at various frequencies is not directly proportional to the DOS, the depolarized IDID Raman spectrum is still closely related to the DOS.

The preceding discussion is based on DOS obtained from zero temperature configurations of the system, since the normal modes and frequencies were calculated at a potential energy minimum. We discuss briefly below the effect of temperature on the DOS and on the related effect on the Raman spectra.

As described earlier, when we consider a system in a potential energy minimum configuration, normal mode analysis of dynamics is straightforward. At finite temperature, however, the notion of normal modes is not very obvious. In spite of this, there has been much progress recently in understanding liquid state dynamics in terms of finite temperature DOS. In particular, the presence of imaginary frequencies (corresponding to the negative curvature of the potential energy surface along some directions at the phase space point defining the system) has been used to obtain information regarding such quantities as diffusion and the velocity autocorrelation function.[13]

Hence, we proceed to calculate the DOS for our system

at finite temperature. The resulting DOS is shown in Fig. 5. The imaginary frequencies are shown on the negative axis, following the convention of Ref. 13. The important feature to notice is that there is no longer a discernible peak around 280 cm^{-1}. Further, there is no clear separation between the translational DOS below 400 cm^{-1} and the librational DOS above. To separate the translational and librational contributions to the DOS, we use the procedure of assigning each mode partially to the translational DOS and librational DOS, based on the squared amplitudes of the corresponding coordinates (all COM coordinates for the translational and all rotational for the librational). The resulting translational DOS is also shown in Fig. 5. Even though there is still no clear peak, we see a broad shoulder to the 80 cm^{-1} peak on the higher side which we interpret to be a largely diminished but still present peak corresponding to the 280 cm^{-1} peak in the quenched DOS. Indeed, even in the Raman data shown in Fig. 1 the peak in the finite temperature MD spectrum is much smaller than in the spectrum calculated from normal modes.

By comparing the zero and finite temperature DOS in Fig. 5, we see that, while the low frequency peak does not change much with temperature, the 280 cm^{-1} peak is significantly altered at finite temperature. We interpret the diminishing of the 280 cm^{-1} peak at finite temperature as due to significant changes on the potential energy surface along normal modes with frequencies in the 280 cm^{-1} region. It will be great interest to study in detail this characteristic change in the potential energy surface and its relation to transitions between potential energy minima that occurs at finite temperatures. In addition to its intrinsic interest, it should shed light on the problem addressed in this paper, namely, the relationship between Raman spectra and the vibrational density of states. A complete understanding of this relationship can only be achieved when one is able to construct the finite-temperature spectrum directly from the finite-temperature DOS. A method for such a calculation has not yet been fully developed, though progress has been made in that direction recently.[22,23]

V. CONCLUSIONS

We have calculated depolarized DID Raman spectra from MD simulations and from the analysis of normal modes of quenched configurations. The normal mode calculations allow us to make comparisons of the spectra with the inherent vibrational states of the liquid. Such a comparison in the present case reveals that the density of vibrational states determines the IDID spectrum to a large extent. The intensity of the 230 cm^{-1} peak in the MD spectrum is smaller than that of the 270 cm^{-1} normal mode peak. We suggest that this discrepancy may be accounted for by the decrease in amplitude of the 280 cm^{-1} peak in the DOS with temperature, which compensates the enhanced "Raman activity" of modes in this frequency range observed in the Raman spectrum for quenched modes. Further study may be needed to fully elucidate the detailed quantitative relationship between the finite temperature DOS and dynamic correlations such as correlations of polarizability studies here.

ACKNOWLEDGMENTS

We thank R. Bansil, T. Keyes, E. Martorana, and M. A. Ricci for helpful discussions, and BP and NSF for support.

[1] G. Walrafen, in *Water: A Comprehensive Treatise, Vol. 1*, edited by F. Franks (Plenum, New York, 1972).
[2] S. Krishnamurthy, R. Bansil, and J. Wiafe-Akenten, J. Chem. Phys. **79**, 5863 (1983).
[3] G. Walrafen, M. S. Hokambadi, and W.-H. Yang, J. Chem. Phys. **85**, 6970 (1986).
[4] P. Benassi, V. Mazzacurati, M. Nardone, M. A. Ricci, G. Ruocco, A. De Santis, R. Frattini, and M. Sampoli, Mol. Phys. **62**, 1467 (1987).
[5] P. A. Madden and R. W. Impey, Chem. Phys. Lett. **123**, 502 (1986).
[6] R. Bansil, T. Berger, K. Toukan, M. A. Ricci, and S. H. Chen, Chem. Phys. Lett. **132**, 165 (1986).
[7] R. Frattini, M. Sampoli, M. A. Ricci, and G. Ruocco, Chem. Phys. Lett. **141**, 297 (1987).
[8] M. A. Ricci, G. Ruocco, and M. Sampoli, Mol. Phys. **67**, 19 (1989).
[9] V. Mazzacurati, M. A. Ricci, G. Ruocco, and M. Sampoli, Chem. Phys. Lett. **159**, 383 (1989).
[10] F. Sciortino and G. Corongiu, Mol. Phys. **79**, 547 (1993).
[11] F. H. Stillinger and T. A. Weber, Phys. Rev. A **25** 978, (1982); J. Phys. Chem. **87**, 2833 (1983); T. A. Weber and F. H. Stillinger, J. Chem. Phys. **80**, 2742 (1984).
[12] F. Sciortino, A. Geiger, and H. E. Stanley, Phys. Rev. Lett. **65**, 3452 (1990).
[13] B. Madan, T. Keyes, and G. Seeley, J. Chem. Phys. **92**, 7565 (1990); **94**, 6762 (1991).
[14] F. Sciortino and S. Sastry, J. Chem. Phys. **100**, 3881 (1994).
[15] W. L. Jorgensen, J. Chandrasekhar, J. D. Madura, R. W. Impey, and M. L. Klein, J. Phys. Chem. **79**, 926 (1983).
[16] H. J. C. Berendsen, J. P. M. Potsma, W. F. van Gunsteren, A. DiNola, and J. R. Haak, J. Chem. Phys. **81**, 3684 (1984).
[17] The temperature is reduced by successively equilibrating the system at 100 K for 20 ps, 10 K for 20 ps, at 1 K for 10 ps and finally 0.000 01 K for 10 ps. At 100 K, there is effectively no diffusion, but the temperature is high enough to allow for motion toward the potential energy minimum during the simulation period. The schedule of temperature equilibration described here anneals the system to the potential energy minimum.
[18] Our purpose is to compare the spectra obtained from MD to the spectra obtained from the normal modes of the same system. Hence, the above restriction does not pose a serious problem.
[19] A. De Lorenzi, A. De Santis, R. Frattini, and M. Sampoli, Phys. Rev. A **33**, 3900 (1986).
[20] W. F. Murphy, J. Chem. Phys. **67**, 5877 (1977).
[21] In experiments, it is observed that the peak positions move to higher values as the temperature is lowered. The shift seen here may be interpreted similarly since the quenched configurations are obtained by minimizing the potential energy of finite-temperature liquid configurations.
[22] M. Buchner, B. M. Ladanyi, and R. M. Stratt (preprint).
[23] T.-M. Wu and R. F. Loring (preprint)